

Explicit kinetic heterogeneity: mechanistic models for interpretation of labeling data of heterogeneous cell populations

Vitaly V. Ganusov^{†‡1}, José A.M. Borghans[§], Rob J. De Boer[‡]

[‡]Theoretical Biology, Utrecht University, Padualaan 8, 3584 CH, Utrecht, The Netherlands

[§]University Medical Center Utrecht, Lundlaan 6, 3584 EA Utrecht, The Netherlands

[†]Institute of Biophysics, Krasnoyarsk, Russia 660036

November 11, 2021

¹Current address: Theoretical Biology and Biophysics, Los Alamos National Laboratory, Los Alamos, NM 87545, USA

Abstract

Estimation of division and death rates of lymphocytes in different conditions is vital for quantitative understanding of the immune system. Deuterium, in the form of deuterated glucose or heavy water, can be used to measure rates of proliferation and death of lymphocytes in vivo. Inferring these rates from labeling and delabeling curves has been subject to considerable debate with different groups suggesting different mathematical models for that purpose. We show that the three models that are most commonly used are in fact mathematically identical and differ only in their interpretation of the estimated parameters. By extending these previous models, we here propose a more mechanistic approach for the analysis of data from deuterium labeling experiments. We construct a model of “kinetic heterogeneity” in which the total cell population consists of many sub-populations with different rates of cell turnover. In this model, for a given distribution of the rates of turnover, the predicted fraction of labeled DNA accumulated and lost can be calculated. Our model reproduces several previously made experimental observations, such as a negative correlation between the length of the labeling period and the rate at which labeled DNA is lost after label cessation. We demonstrate the reliability of the new explicit kinetic heterogeneity model by applying it to artificially generated datasets, and illustrate its usefulness by fitting experimental data. In contrast to previous models, the explicit kinetic heterogeneity model 1) provides a mechanistic way of interpreting labeling data; 2) allows for a non-exponential loss of labeled cells during delabeling, and 3) can be used to describe data with variable labeling length.

Classification: Immunology, Mathematical Biology.

Keywords: *D-glucose, parameter estimation, cell turnover, lymphocyte dynamics, heavy water*

Short title: Measuring cell turnover

Abbreviations: D-glucose = 2H_2 -glucose, heavy water = 2H_2O , KH = kinetic heterogeneity, AM = asymptote model, RSS = residual sum of squares.

1 Introduction

There is little consensus about the expected life spans of lymphocyte populations in health and disease. Labeling the DNA of dividing cells with deuterium has proved to be one of the most reliable and feasible ways to study the population dynamics of lymphocytes in healthy human volunteers and in patients (1, 2, 3). Deuterium, in the form of deuterated glucose or heavy water, is used to measure the rate at which cells are dividing *in vivo*, without the need to interfere with these cellular kinetics. Deuterium is incorporated into newly synthesized DNA via the *de novo* pathway (4), and enrichment of deuterium (over hydrogen) in the DNA of cells is therefore related to cell division. During label administration, the fraction of deuterium-labeled nucleotides increases over time, and after label withdrawal, the fraction generally declines over time (2, 3). Labeling DNA with deuterium in humans has a number of clear advantages over other labeling techniques such as with BrdU, including the absence of toxicity, the fact that the rate of incorporation of deuterium into the DNA is independent of the amount of nucleotides present, and a simpler mathematical interpretation of the data (4, 5, 6). Several mathematical models have been proposed for estimation of cellular turnover rates from labeling data (reviewed in (7)), including a simple precursor-product relationship (1), a source model (2), a two-compartment model (8, 9), and a kinetic heterogeneity model (10).

In their pioneering study on deuterium labeling, Mohri et al. (2) found that the estimated rate of cell proliferation was typically smaller than the rate of cell death. Because the cell population under investigation was in steady state, the extra death must be compensated by a source of cells, for example from the thymus. This interpretation was challenged by the work of Asquith et al. (10), which pointed out that estimated proliferation and death rates do not have to be equal if the population is kinetically heterogeneous (i.e., different cells in the population divide and die at different rates). Because the labeled population preferentially contains cells that proliferate (and die) relatively rapidly, the estimated rate of cell death is in fact expected to be higher than the average proliferation rate (10).

Here we extend these studies and propose a more mechanistic approach to estimate the rates of lymphocyte proliferation and death from deuterium labeling experiments. First, we show that the three most commonly used mathematical models are in fact kinetically identical (i.e., will lead to identical estimates of the average rate of cell turnover), and only differ in their biological interpretation of the model parameters. Second, we formulate a novel mathematical model which explicitly takes into account kinetic heterogeneity of lymphocyte populations, and show how lymphocyte turnover rates can be calculated using this model. Several previously made experimental observations arise naturally from the new model. For example, we find that the rate of label loss during delabeling generally exceeds the rate of label accumulation during the labeling phase. Our model also explains the dependence of the rate at which labeled DNA is lost after label withdrawal on the duration of the labeling period (10). As a proof of principle, we demonstrate that the newly developed model can fit artificially generated data,

and correctly returns their underlying kinetic parameters. We also illustrate the usefulness of the new model by fitting it to several experimental datasets. The novel explicit kinetic heterogeneity model may offer alternative interpretations of how infections or treatments affect the turnover of human lymphocytes *in vivo*.

2 Results

2.1 Previous models

Although different models have been proposed for interpretation of deuterium labeling data (2, 10) and are being debated in the literature, they are in fact mathematically identical. Following De Boer et al. (11), consider a cell population consisting of a fraction α of cells with average turnover rate d (i.e., an expected life span of $1/d$ days), and a fraction $1 - \alpha$ of cells that do not turnover at all on the time scale of the experiment. During the labeling phase, consider the fraction of unlabeled DNA U_α in the sub-population with death rate d . Because DNA is only lost by cell death, U_α changes according to:

$$dU_\alpha/dt = -dU_\alpha.$$

During the delabeling phase the fraction of labeled DNA in that same population (L_α) is described by:

$$dL_\alpha/dt = -dL_\alpha,$$

because labeled DNA can only be lost by cell death. Since $U_\alpha + L_\alpha = 1$, the fraction of labeled DNA in the whole population $L(t) = \alpha L_\alpha(t)$ is described by:

$$L(t) = \begin{cases} \alpha (1 - e^{-dt}), & \text{if } t \leq T, \\ L(T)e^{-d(t-T)}, & \text{otherwise,} \end{cases} \quad (1)$$

where T is the duration of the labeling period. Given that only a fraction α of all cells in the population are turning over (or dying) at rate d , the average turnover rate of the whole population is $\alpha \times d$ (11). Importantly, this approach does not require us to describe how new cells are formed, i.e., they could be generated by the thymus and/or by proliferation. Extending this model by assuming n sub-populations with different rates of cell proliferation p_i and death d_i , and possibly generation of new cells from a source s_i (Figure 1), the fraction of labeled nucleotides in the whole population at time t is given by:

$$L(t) = \begin{cases} \sum_{i=1}^n \alpha_i (1 - e^{-d_i t}), & \text{if } t \leq T, \\ \sum_{i=1}^n \alpha_i (1 - e^{-d_i T}) e^{-d_i(t-T)}, & \text{otherwise,} \end{cases} \quad (2)$$

where α_i is the fraction of cells in population i with death rate d_i , and $\alpha = \sum_{i=1}^n \alpha_i \leq 1$ is the asymptote that would be approached if label would be administered indefinitely.

The “source” model that was previously proposed by Mohri et al. (2) considered one homogeneous cell population, but allowed for a source of unlabeled cells during the labeling phase, i.e., $dU/dt = s_U - dU$, which also gives rise to an asymptote $\alpha = 1 - \hat{s}_U/d$, defining the fraction of cells that can maximally become labeled (here $\hat{s}_U = s_U/X$ where X is the total number of cells in the population at equilibrium and s_U is the number of cells with unlabeled DNA coming from the source per day during the labeling phase (2)). Mathematically, the source model is therefore identical to eqn. (1). Similarly, in the kinetic heterogeneity model devised by Asquith et al. (10), $dL/dt = p(U + L) - dL = p - dL$ for the labeling phase and $dL/dt = -dL$ for the delabeling phase. Assuming $p \leq d$ one again obtains eqn. (1) with $\alpha = p/d$. Therefore, all these models are mathematically identical and only differ in the biological interpretation of their model parameters (see also (12)). We propose to call all these models the “asymptote model”. Importantly, in all models the product $\alpha \times d$ can be interpreted as the average rate of cell turnover of the population as a whole (11), and therefore, all three models, when fitted to data, will deliver identical estimates of the average turnover rate, which is the parameter of interest.

2.2 Kinetic heterogeneity model with continuously distributed turnover rates

Because of its simplicity, the model given in eqn. (1) has two limitations. First, the asymptote level is a phenomenological parameter that depends on the length of the labeling period (10). As a consequence, datasets with different labeling periods will likely give rise to different estimated asymptotes and different estimated average rates of cell turnover. Therefore strictly speaking, this model cannot be used to explain multiple datasets coming from the same experimental setup varying only in the length of the labeling period; the differences in the rate at which labeled DNA is lost would force either the asymptote or the estimated average turnover rate to be different for the different labeling periods (Den Braber et al. in preparation). Second, the model assumes that the increase in labeled DNA during the uplabeling phase, and the loss of labeled DNA during the delabeling phase can be described by single exponentials. This may be incorrect if cell populations with different turnover rates are labeled and subsequently lost.

Under very general assumptions, we have formulated an alternative model that does not make these *a priori* assumptions. In our new model, a cell population consists of n sub-

populations each with different kinetic properties (see Figure 1 and eqn. (2)). If the number of sub-populations is large ($n \rightarrow \infty$), the sum in eqn. (2) can be replaced by an integral. The fraction of labeled nucleotides in the population then becomes (see Supplemental Information for derivation)

$$L(t) = \int_0^\infty L(t, d) dd \quad (3)$$

where $L(t, d)$ is given by eqn. (1) where $\alpha = f(d)$ is the frequency distribution of turnover rates, and $f(d)dd$ is the probability that a randomly chosen cell in the population belongs to a sub-population with a turnover rate in the range $(d, d + dd)$. If the turnover rates in the population, $f(d)$, follow a gamma distribution, the change in the fraction of labeled DNA with time is given by:

$$L(t) = \begin{cases} 1 - \left(1 + \frac{\bar{d}t}{k}\right)^{-k}, & \text{if } t \leq T, \\ \left(1 + \frac{\bar{d}(t-T)}{k}\right)^{-k} - \left(1 + \frac{\bar{d}t}{k}\right)^{-k}, & \text{otherwise,} \end{cases} \quad (4)$$

where \bar{d} is the average rate of cell turnover in the population, k is the shape parameter of the gamma distribution, and T is the duration of the labeling period. For $k = 1$, the gamma distribution becomes an exponential distribution, and the rate at which the fraction of labeled DNA changes is simply:

$$L(t) = \begin{cases} \frac{\bar{d}t}{1+\bar{d}t}, & \text{if } t \leq T, \\ \frac{\bar{d}T}{(1+\bar{d}t)(1+\bar{d}(t-T))}, & \text{otherwise.} \end{cases} \quad (5)$$

This is an interesting model in which a single parameter \bar{d} predicts both the rate of uplabeling and downlabeling, and in which there is no asymptote below 100% for the level of labeled DNA, i.e., under continuous label administration all cells in the population will become labeled (Figure 2). Moreover, this model predicts that the initial rate d^* at which labeled DNA is lost after label cessation depends on the duration of the labeling period, $d^* \approx \bar{d}(1 + (1 + \bar{d}T)^{-1})$ (see Supplementary Information for derivation). According to this model, short labeling experiments ($\bar{d}T \ll 1$, $d^* \approx 2\bar{d}$) will lead to 2-fold faster initial rates of decline in the fraction of labeled nucleotides than longer labeling experiments ($\bar{d}T \gg 1$, $d^* \approx \bar{d}$).

Solutions (4) and (5) predict that the initial rate of increase in the fraction of labeled DNA is the average rate of cell turnover \bar{d} (see also Supplementary Information). However, the increase in the fraction of labeled DNA does not appear to be exponential, as was implicitly assumed

in the asymptote models discussed above. Similarly, during the delabeling period, the model predicts a non-exponential decline in the fraction of labeled DNA (Figure 2 and 3). In general, the initial rate of label loss during delabeling d^* is given by:

$$d^* \approx \bar{d} + \frac{\text{var}(d)}{\bar{d}}, \quad (6)$$

where $\text{var}(d)$ is the variance of the distribution of turnover rates in the population. In case when turnover rates follow a gamma distribution, the initial rate of loss of the label after short labeling periods depends on the shape parameter k of the distribution, $d^* \approx \bar{d}(1 + 1/k)$, while it does not after long labeling periods ($d^* \approx \bar{d}$). The rate of loss of labeled DNA slows down as less DNA remains labeled, which is most clearly seen when proliferation rates are distributed according to a very skewed gamma distribution ($k < 1$, Figure 3). This is a natural property of the explicit kinetic heterogeneity model as loss of labeled DNA is reflecting the distribution of the turnover rates of the different sub-populations, with labeled DNA from the most rapidly turning over sub-populations being lost first (early fast decline) and labeled DNA from the other, more slowly turning over, populations being lost later (late slow decline).

To study the effect of the shape of the turnover rate distribution on the predicted labeling curve, we plotted the changes in the fraction of labeled DNA as predicted by the model (Figure 3A&B) with different gamma-distributed turnover rates (Figure 3C). When the gamma distribution is highly skewed (i.e., $k < 1$), the majority of cell sub-populations have very low rates of cell turnover, and the average rate of cell turnover is dominated by a few sub-populations that turn over unrealistically fast. This is best illustrated by calculating the cumulative contribution of a sub-population with a particular rate of turnover to the average turnover rate of the population \bar{d} (Figure 3D):

$$\beta(d) = \frac{1}{\bar{d}} \int_0^d x f(x) dx. \quad (7)$$

For large values of the shape parameter k (e.g., $k = 5$), the sub-populations with turnover rates that are close to the average turnover rate \bar{d} , are the main contributors to the average rate of cell turnover (Figure 3D). When the gamma distribution is extremely skewed ($k = 0.01$), the rate of turnover of the sub-populations that contribute significantly to the average turnover rate is as high as $10^1 - 10^2$ per day, which is biologically unrealistic. Therefore, the gamma distribution should be rejected whenever one estimates a high average turnover rate \bar{d} with a highly skewed gamma distribution (i.e., a low value of the shape parameter k). As a rule of thumb, k should be larger than 0.1 (Figure 3D); otherwise a relatively large fraction of sub-populations has unrealistically high turnover rates.

It is possible, however, that not all cells in the population are turning over. The models above can easily be extended to incorporate this possibility by allowing for the same asymptote as in eqn. (1). An example would be a labeling experiment in which slowly turning over naive T lymphocytes and more rapidly turning over memory lymphocytes are not separated (2). If only a fraction α of cells have turnover rates that are distributed exponentially, and the other cells undergo negligible turnover on the time scale of the experiment, the change of the fraction of labeled nucleotides with time is given by:

$$L(t) = \begin{cases} \frac{\alpha \bar{d}_\alpha t}{1 + \bar{d}_\alpha t}, & \text{if } t \leq T, \\ \frac{\alpha \bar{d}_\alpha T}{(1 + \bar{d}_\alpha t)(1 + \bar{d}_\alpha (t - T))}, & \text{otherwise,} \end{cases} \quad (8)$$

where \bar{d}_α is the average of the exponentially distributed turnover rates, and the average rate of cell turnover in the whole population is $\bar{d} = \alpha \bar{d}_\alpha$.

It should be noted that the results of this section are applicable both to proliferating and non-proliferating lymphocytes, given the general structure of the cell population in the model (see Figure 1). As a downside of this, the model does not allow to estimate which fraction of labeling of lymphocytes is due to proliferation of precursors (e.g., thymocytes for naive T cells) or due to peripheral proliferation of the lymphocyte population itself. Additional experiments, such as thymectomy in case of studies of naive T-cell turnover, may allow to estimate the separate contribution of peripheral T-cell proliferation (13, Den Braber et al. submitted).

2.3 Fitting artificial data to validate the model

Having analytical expressions for several kinetic heterogeneity models, we analyzed how well these models can recover the (known) average turnover parameter from simulated (artificial) datasets. Three models were used to generate artificial datasets: 1) the kinetic heterogeneity model with gamma-distributed rates of turnover (eqn. (4)), referred to as the ‘‘Gamma model’’, 2) the kinetic heterogeneity model in which a fraction $\alpha \leq 1$ of cells have exponentially-distributed rates of turnover (eqn. (8)), referred to as the ‘‘Exponential model’’, and 3) a ‘‘Two population model’’ (eqn. (2) with $n = 2$, turnover rates d_1 and d_2 , average turnover rate $\bar{d} = \alpha d_1 + (1 - \alpha)d_2$, and $d_1 > \bar{d}$). These datasets were subsequently fitted by the same three models as well as by the conventional Asymptote model (eqn. (1)).

Not surprisingly, the models delivered correct estimates for the average turnover parameter if a dataset was fitted with the model that was used to generate the data (Table 1 and Figure 5; with the results obtained by fitting the Two population model not shown). All models described the data sets generated by the other models reasonably well (Figure 4), although some features in the data could not be reproduced. For example, the Asymptote model failed to describe the

decreasing rate at which labeled DNA is lost over time, which is observed in the data generated by the Gamma and the Exponential models (see last data points in Figure 4). Some model fits delivered incorrect estimates for the average turnover rate if the data were generated using another model. For example, the Gamma model overestimated the average turnover rate when the data were generated using the Exponential model (up to 2-fold), and underestimated \bar{d} for data generated using the Two populations model (over 2-fold). This is most likely due to the strong constraint of the model that both uplabeling and delabeling curves have to be described with one mechanism, i.e., gamma-distributed turnover rates. On the other hand, the Asymptote model always underestimated the true average turnover rate (up to 2-fold for data generated by the Two-populations model; Table 1). It did perform somewhat better than the Gamma model as judged by the mean square distances, because the rate of uplabeling and downlabeling are relatively independent in the Asymptote model.

Given that natural lymphocyte populations are likely to contain resting sub-populations, some extent of saturation in the fraction of deuterium-labeled nucleotides is expected in almost any experimental dataset. In our artificial data, such an asymptote was imposed when using the Exponential model by letting only 50% of all cells to turn over (Figure 4 and Table 1). It is therefore not surprising that the Gamma model, which does not have an explicit asymptote in the uplabeling phase (see eqn. (4)), did not correctly estimate the average turnover rate for the data generated by the Exponential model (Figure 5). Extending the Gamma model to allow for an explicit asymptote during the labeling phase (α) indeed improved the estimate of the average turnover rate $\bar{d} = \alpha \bar{d}_\alpha = 0.13 \text{ day}^{-1}$ (with 95% CIs = $0.095 - 0.22 \text{ day}^{-1}$ which includes the true average $\bar{d} = 0.1 \text{ day}^{-1}$), even though the estimated fraction of turning over cells α was not significantly different from 1 (i.e., an F-test would not reject a model with $\alpha = 1$; results not shown). This exercise illustrates that when fitting experimental data one should check whether allowing for an explicit asymptote in the uplabeling phase leads to different estimates of the average turnover rate. Interestingly, all models underestimated the average rate of cell turnover when the data were generated using the Two populations model. This is because the models did not reproduce the relatively rapid accumulation of the labeled DNA in the first days (Figure 4). Fitting the Two populations model to these data led to better estimates of the average turnover rate ($\bar{d} = 0.084$ per day with 95% CIs = $(0.062 - 0.35)$ for 7 days of labeling, and $\bar{d} = 0.26$ per day with 95% CIs = $(0.061 - 0.44)$ for 15 days of labeling, where the constant $\bar{d} = 0.1 \text{ day}^{-1}$ is contained within both ranges, results not shown).

Although stable isotope labeling seems to be the best tool at hand to estimate rates of lymphocyte turnover, a recent review (7) pointed out that estimated lymphocyte turnover rates differ consistently, depending on the labeling method used (heavy water or deuterated glucose), and the length of the labeling period. *A priori*, according to the Asymptote model that is generally used, the estimated average turnover rate should not depend on the length of the labeling period. Using our explicit kinetic heterogeneity models, we analyzed the influence of the length of the labeling period on the estimated average turnover rate. For all models, we found that the duration of labeling had little influence on the estimated average turnover

rate (for the chosen labeling periods of 7 and 15 days, Table 1). This suggests that longer labeling periods will not necessarily result in lower estimates of the average cell turnover rate than shorter labeling periods.

An overall conclusion of this analysis is that without a good understanding of the underlying model of cell proliferation (i.e., the distribution of turnover rates in the population), one may obtain incorrect estimates of cellular turnover rates, even if the quality of the fit to the data is acceptably good. Therefore, when analyzing experimental data, one should aim at using several alternative models for fitting, and investigate whether estimates of kinetically important parameters, such as the average rate of cell turnover, are independent of the model used.

2.4 Fitting experimental data

We next sought to determine how well the new kinetic heterogeneity models fit experimental data. Using deuterated glucose, Mohri et al. (2) obtained labeling data of T lymphocytes from uninfected healthy human volunteers and from chronically HIV-infected patients. Previously, these data were fitted using an extended 4-parameter source model, to estimate the rates of cell division and death of T lymphocytes in healthy humans, and to obtain insights into how these rates change upon HIV-infection (2). Lymphocytes were sorted into CD4⁺ and CD8⁺ T cells, without distinguishing between their naive and memory subpopulations. Since naive T cells have a much slower rate of turnover than memory T cells (3), it is natural to assume an asymptote in the fraction of labeled nucleotides of unsorted CD4⁺ and CD8⁺ T cells.

We have refitted the labeling data from the four healthy human volunteers studied by Mohri et al. (2), again using the three models for cell proliferation: the Asymptote model (eqn. (1)), the Exponential model (with a fraction α of cells with exponentially distributed turnover rates, eqn. (8)) and the Gamma model (with gamma distributed turnover rates, eqn. (4)). The data were fitted simultaneously for all four healthy volunteers while searching for the minimal number of parameters that describe the data with reasonable quality (using a partial F-test for nested models (14)). Overall, the models described the data reasonably well (Figure 6 and Table 2 and 3). For CD4⁺ T cells, the average turnover rate and the delay at which labeled cells appeared in the blood did not differ significantly between patients (Table 2). For all patients, the average rate of turnover was about 0.46% per day with a corresponding estimated half-life of $\ln 2/\bar{d} \approx 151$ days. There was an average delay of one day before labeled cells appeared in the blood. The average turnover rate of CD4⁺ T cells from control c1 was always higher than that of the other individuals, irrespective of the model used (Figure 7A), which may be a sign of an immune response to an infection in c1 (see also below). Both the Asymptote model ($\alpha \approx 15\%$) and the Exponential model ($\alpha \approx 25\%$) predicted an asymptote in labeling that is smaller than the fraction of memory phenotype CD4⁺ T cells in humans of that age (3). The Gamma model could describe these data even better than the other two models with no need

for an asymptote. The observation that the estimate of the asymptote can differ dramatically between different models reconfirms our statement that this parameter is of little use for data interpretation (11).

For CD8⁺ T cells, the parameters differed significantly between different healthy volunteers, with the exception of the asymptote level α in the Exponential model which could be fixed between individuals. The estimates of the average turnover rates of CD8⁺ T cells in healthy volunteers c2–c4 did not strongly depend on the model that was used to fit the data. However, the estimated turnover rate of CD8⁺ T cells in individual c1, which was much higher than the estimated turnover rate in the other healthy volunteers, depended strongly on the model used and was estimated to be the highest when using the Gamma model. The latter model fitted the labeling data from all four individuals very well and reproduced the non-exponential change in the fraction of labeled DNA in the downlabeling phase (Figure 6F). In all four healthy individuals, CD8⁺ T cells turned over at a slower rate than CD4⁺ T cells; the average turnover rate of CD8⁺ T cells was $\bar{d} = 0.29\%$ per day with a corresponding half-life of $\ln 2/\bar{d} \approx 239$ days. The fits of the Asymptote model and the Exponential model predicted an asymptote in labeling of $\alpha \approx 0.15$ (Table 3). Even though the Gamma model lacks an explicit asymptote lower than 1, it fitted these data with equally good quality as the models with explicit asymptotes. Allowing for an explicit asymptote in the Gamma model did not improve the quality of the fit (CD4⁺ T cells: $p > 0.38$, CD8⁺ T cells: $p > 0.99$, F-test), and the estimated average lymphocyte turnover rates were not affected by the addition of an explicit asymptote (results not shown).

It is important to investigate whether the good description of the data of the model with gamma distributed turnover rates is achieved with biologically reasonable parameter values. In all data we estimated the shape parameter of the gamma distribution to be small, i.e. $k < 1$, but k was estimated to be larger than 0.1 in seven of the eight fits. Low values of the shape parameter k imply that in the population most cells turn over at very slow rates while a few populations turn over very rapidly. To investigate whether such a distribution is biologically reasonable, we calculated the fraction of cells in the population with a turnover rate higher than $d_{max} = 1$ per day which is the maximal rate of CD8⁺ T-cell proliferation in rhesus macaques (15). This fraction is given by $\int_{d_{max}}^{\infty} f(d)dd$ for the estimated parameters of the distribution (see Table 2 and 3). For most fits, the fraction of cells with turnover rates higher than 1 per day is $\leq 10^{-11}$, and given the estimated total number of lymphocytes in humans of $\sim 10^{12}$ (16), that would yield only a few cells with unrealistically high rates of turnover. However, for the CD8⁺ T cells of healthy volunteer c1 we found that $\sim 3 \times 10^{-5} \times 10^{12} = 3 \times 10^7$ cells turn over at rates higher than 1 per day, which is unrealistically high.

To investigate this further we reanalyzed the CD8⁺ T-cell labeling data of individual c1 using several extended models. In the first model, a fraction α of cells in the population have gamma-distributed turnover rates while the other fraction $(1 - \alpha)$ of cells turn over at the highest possible rate $d_{max} = 1 \text{ day}^{-1}$. This situation may correspond to a scenario where a small fraction of CD8⁺ T cells is responding to an infection. However, this model failed to

describe the data with biologically reasonable parameter values ($\alpha \approx 1$ and $k = 0.03$).

In the second extended model, the gamma distribution of turnover rates was truncated at a maximal value $d_{max} = 1$ (see Supplementary Information for analytical results). The fit of this model to the labeling data for individual c1 was of similar quality as the fit in which the gamma distribution was not truncated, and it delivered similar estimates for the average turnover rate and the shape parameter ($\bar{d} = 0.66\%$ per day and $k = 0.030$, results not shown). We estimate that in healthy volunteer c1 about 0.1% of all CD8⁺ T cells are turning over rapidly at rates between 0.5–1.0 per day, which is reasonable. For example, in mice responding to lymphocytic choriomeningitis virus (LCMV) infection, at the peak of the immune response more than 50% of all CD8⁺ T cells in the spleen are specific for the virus (17, 18).

Finally, in the third model, we assumed that the CD8⁺ T-cell population in patient c1 consists of naive, memory and effector T-cell subpopulations with 3 different rates of turnover (see eqn. (2) with $n = 3$). Assuming that the rate of turnover of naive T cells is 0 and that letting for effector cells $d_{max} = 1$ per day, we could obtain excellent fits of the labeling data with an estimated average turnover rate $\bar{d} = 1.4\%$ per day (95% CIs = (1.2 – 1.6)% per day) which is much higher than estimates obtained by other models (Figure 7). Using model selection methods such as the Akaike Information Criterion, we found equal support for the latter model and the model in which the turnover rates follow a truncated gamma distribution (19, results not shown). We can conclude, therefore, that the average turnover rate of CD8⁺ T cells in patient c1 is at least 0.62% per day (Gamma model) and could be as high as 1.4% per day (Three population model). In summary, it seems that the average turnover rate of both CD4⁺ and CD8⁺ T cells was increased in individual c1 as compared to other individuals, and this could be explained by a normal immune response in this otherwise healthy volunteer.

3 Discussion

In this paper we have analyzed the models that are commonly used in the literature to estimate the rates of cell turnover from deuterium labeling data. We have shown that the three most commonly used models are mathematically identical and therefore provide identical fits to the data, and only differ in the biological interpretation of the estimated parameters (12). The simplest summary of labeling data is provided by a model that has two parameters: d as the rate of cell death in the population, and α as the fraction of cells that undergo turnover, which determines the asymptote of the uplabeling phase (see eqn. (1)). In this model, $\alpha \times d$ gives the estimated average rate of cell turnover. We have extended this model by allowing for multiple sub-populations i of size α_i with different turnover rates d_i (see eqn. (2)). This extended model can be used to investigate potential heterogeneity of cell populations, by fitting labeling data with a model that has one, two, or more sub-populations with different turnover rates. Using standard techniques of model selection (e.g., the partial F-test or the Akaike Information

Criterion), one can investigate which of those models describes the labeling data best, given the number of model parameters (14, 19), or one can study whether the estimated average turnover rate is converging to an invariant value by increasing the number of compartments (work in progress).

For the case where the number of sub-populations is large, we derived a model with continuous kinetic heterogeneity. For several continuous distributions such as the exponential and the gamma distribution, the model predicts that the initial rate of loss of labeled DNA after label withdrawal is determined by the duration of the labeling period as has been observed experimentally (10). Moreover, in the model the average turnover rate, which determines the initial rate of label accumulation in the population, turned out to be independent of the length of the labeling period. However, it should be noted that the average rate of cell turnover that is estimated from experimental data using, for example, the Asymptote model, may in fact depend on the duration of labeling (7, Den Braber et al. (in preparation)). Potential reasons for this discrepancy will be investigated in more detail elsewhere.

Previous models had certain artifacts: the asymptote labeling level was dependent on the length of the labeling period, and the accrual of labeled DNA during the uplabeling phase and the loss of labeled DNA during the downlabeling period were always described by single exponential functions. It is, therefore, unclear whether such limited models provide a good description of truly kinetically heterogeneous populations. Although at first glance it may seem impossible to fit labeling data with models that contain an infinite number of sub-populations with different rates of turnover, we have shown that this is in fact feasible. By fitting artificial labeling data, we have validated these new models: they generally give good fits to the data and converge on average turnover rates that are close to the known average turnover rate. Moreover, the new explicit heterogeneity model outperformed the Asymptote model when it came to fitting experimental data, especially when the rates of label accumulation and loss are not exponential (see Figure 6). Importantly, due to its relatively general structure, all results of the kinetic heterogeneity model are applicable to both non-proliferating and proliferating lymphocytes, all having a distribution of turnover values (results not shown). Moreover, because the model naturally incorporates the dependence of the rate of label loss on the length of the labeling period, this is the first model that can be strictly applied to fit labeling data with different labeling periods.

We have focused our analysis on a particular type of kinetic heterogeneity in which kinetic properties of cells of a given subpopulation do not change over time and there is no exchange of cells in different subpopulations. However, in some circumstances, such as during an immune response, this assumption may be violated since over the course of infection, lymphocytes do change their kinetic properties over time (e.g., (20)). Taking into account such a type of *temporal* heterogeneity is therefore biologically justified. We have shown that estimates of the average turnover rate of the population may depend on the model used (e.g., Figure 4 and 7B); it is therefore important to develop additional (simple) models that take temporal heterogeneity

of cell populations into account (21, 22). We propose that future studies should aim at testing multiple models in how well they describe the labeling data and whether these models deliver similar estimates of important kinetic parameters such as the average rate of cell turnover.

4 Methods

When fitting experimental data, the models were extended to allow for the initial delay in the labeling of cells (see also (2)). For example, including a delay in the Asymptote model (given by eqn. (1)) takes the form

$$L(t) = \begin{cases} 0, & \text{if } t \leq \tau, \\ \alpha(1 - e^{-d(t-\tau)}), & \text{if } \tau < t \leq T + \tau, \\ L(T)e^{-d(t-T-\tau)}, & \text{otherwise.} \end{cases} \quad (9)$$

To normalize the residuals of the model fits to experimental data, given that the data are expressed as proportions, the data and the model predictions were transformed as $\arcsin(\sqrt{x})$ where x is the frequency of labeled DNA in the population (23). The models were fitted according to the least squares method by using the FindMinimum routine in Mathematica. Confidence intervals were calculated by bootstrapping the residuals with 1000 simulations.

References

1. Hellerstein, M., M. B. Hanley, D. Cesar, S. Siler, C. Papageorgopoulos, E. Wieder, D. Schmidt, R. Hoh, R. Neese, D. Macallan, S. Deeks, and J. M. McCune. 1999. Directly measured kinetics of circulating T lymphocytes in normal and HIV-1-infected humans *Nat Med* 5: 83–9.
2. Mohri, H., A.S. Perelson, K. Tung, R.M. Ribeiro, B. Ramratnam, M. Markowitz, R. Kost, A. Hurley, L. Weinberger, D. Cesar, M.K. Hellerstein, and D.D. Ho. 2001. Increased turnover of T lymphocytes in HIV-1 infection and its reduction by antiretroviral therapy. *J Exp Med* 194: 1277–87.
3. Vrisekoop, N., I. den Braber, A. B. de Boer, A. F. Ruiter, M. T. Ackermans, S. N. van der Crabben, E. H. Schrijver, G. Spierenburg, H. P. Sauerwein, M. D. Hazenberg, R. J. de Boer, F. Miedema, J. A. Borghans, and K. Tesselaar. 2008. Sparse production but preferential incorporation of recently produced naive T cells in the human peripheral pool. *Proc Natl Acad Sci U S A* 105: 6115–20.

4. Hellerstein, M.K. 1999. Measurement of T-cell kinetics: recent methodologic advances. *Immunol Today* 20: 438–41.
5. Macallan, D. C., C. A. Fullerton, R. A. Neese, K. Haddock, S. S. Park, and M. K. Hellerstein. 1998. Measurement of cell proliferation by labeling of DNA with stable isotope-labeled glucose: studies in vitro, in animals, and in humans *Proc Natl Acad Sci USA* 95: 708–13.
6. Neese, R.A., S.Q. Siler, D. Cesar, F. Antelo, D. Lee, L. Misell, K. Patel, S. Tehrani, P. Shah, and M.K. Hellerstein. 2001. Advances in the stable isotope-mass spectrometric measurement of DNA synthesis and cell proliferation. *Anal Biochem* 298: 189–95.
7. Borghans, J.A. and R.J. de Boer. 2007. Quantification of T-cell dynamics: from telomeres to DNA labeling. *Immunol Rev* 216: 35–47.
8. Ribeiro, R.M., H. Mohri, D.D. Ho, and A.S. Perelson. 2002. In vivo dynamics of T cell activation, proliferation, and death in HIV-1 infection: why are CD4+ but not CD8+ T cells depleted? *Proc Natl Acad Sci USA* 99: 15572–7.
9. Ribeiro, R.M., H. Mohri, D.D. Ho, and A.S. Perelson. 2002. Modeling deuterated glucose labeling of T-lymphocytes. *Bull Math Biol* 64: 385–405.
10. Asquith, B., C. Debacq, D.C. Macallan, L. Willems, and C.R. Bangham. 2002. Lymphocyte kinetics: the interpretation of labelling data. *Trends Immunol* 23: 596–601.
11. De Boer, R.J., H. Mohri, D.D. Ho, and A.S. Perelson. 2003. Estimating average cellular turnover from 5-bromo-2'-deoxyuridine (BrdU) measurements. *Proc R Soc Lond B Biol Sci* 270: 849–58.
12. Asquith, B., J.A. Borghans, V.V. Ganusov, and D.C. Macallan. 2009. Lymphocyte kinetics in health and disease. *Trends Immunol* .
13. Parretta, E., G. Cassese, A. Santoni, J. Guardiola, A. Vecchio, and F. Di Rosa. 2008. Kinetics of in vivo proliferation and death of memory and naive CD8 T cells: parameter estimation based on 5-bromo-2'-deoxyuridine incorporation in spleen, lymph nodes, and bone marrow. *J Immunol* 180: 7230–9.
14. Bates, D. M. and D. G. Watts. 1988. *Nonlinear regression analysis and its applications*. John Wiles & Sons, Inc. 365 .
15. Davenport, M.P., R.M. Ribeiro, and A.S. Perelson. 2004. Kinetics of virus-specific CD8+ T cells and the control of human immunodeficiency virus infection. *J Virol* 78: 10096–103.
16. Ganusov, V.V. and R.J. De Boer. 2007. Do most lymphocytes in humans really reside in the gut? *Trends Immunol* 28: 514–8.

17. Murali-Krishna, K., J.D. Altman, M. Suresh, D.J.D. Sourdive, A.J. Zajac, J.D. Miller, J. Slansky, and R. Ahmed. 1998. Counting antigen-specific CD8+ T cells: A re-evaluation of bystander activation during viral infection *Immunity* 8: 177–187.
18. Homann, D., L. Teyton, and M.B. Oldstone. 2001. Differential regulation of antiviral T-cell immunity results in stable CD8+ but declining CD4+ T-cell memory. *Nat Med* 7: 913–919.
19. Burnham, K. P. and D. R. Anderson. 2002. *Model selection and multimodel inference: a practical information-theoretic approach*. Springer-Verlag, New York 340 .
20. Antia, R., V.V. Ganusov, and R. Ahmed. 2005. The role of models in understanding CD8+ T-cell memory. *Nat Rev Immunol* 5: 101–111.
21. Grossman, Z., R. B. Herberman, D. S. Dimitrov, I. M. Rouzine, and J. M. Coffin. 1999. T cell turnover in SIV infection *Science* 284: 555a–555d.
22. Grossman, Z., M. Meier-Schellersheim, W.E. Paul, and L.J. Picker. 2006. Pathogenesis of HIV infection: what the virus spares is as important as what it destroys. *Nat Med* 12: 289–95.
23. Hogg, R.V. and A.T. Craig. 1995. *Introduction to Mathematical Statistics* Macmillan.

5 Supplementary Information

5.1 Derivation of the model with continuous kinetic heterogeneity

The average label incorporation in a population consisting of n sub-populations is given by eqn. (2). If the number of sub-populations is large ($n \rightarrow \infty$), one could switch from summation to integration in eqn. (2). If α_i is the fraction of cells in sub-population i with turnover rate d_i , then, as $n \rightarrow \infty$, $\alpha_i = f(d)dd$, where the latter is the probability that a randomly chosen cell from a population will have a turnover rate in the range $(d, d + dd)$. If $\sum_{i=1}^n \alpha_i = 1$, then $f(d)$ is also normalized to 1. Then for $t > T$, eqn. (2) can be rewritten in a different form

$$L(t) = \lim_{n \rightarrow \infty} \left[1 - \sum_{i=1}^n \alpha_i e^{-d_i t} \right] = 1 - \int_0^{\infty} f(d) e^{-dt} dd. \quad (\text{S.1})$$

Similarly, from eqn. (2), during the delabeling period, the fraction of labeled DNA is given by

$$L(t) = \int_0^{\infty} f(d) e^{-d(t-T)} dd - \int_0^{\infty} f(d) e^{-dt} dd. \quad (\text{S.2})$$

One can then calculate several important characteristics that determine the change of the fraction of labeled DNA over time. First, the initial uplabeling rate can be calculated using eqn. (S.1) for small t , yielding

$$L(t) = 1 - \int_0^{\infty} f(d) e^{-dt} dd \approx 1 - \int_0^{\infty} f(d) (1 - dt) dd = \bar{d}t. \quad (\text{S.3})$$

where $\bar{d} = \int_0^{\infty} df(d)dd$, and $\int_0^{\infty} f(d)dd = 1$ by definition. The importance of this result is that it demonstrates that for any distribution $f(d)$, the estimated initial rate of uplabeling is determined only by the average rate of cell turnover.

During delabeling, the initial change in the fraction of labeled DNA (for $t = T + \varepsilon$ with ε relatively small), can be calculated from:

$$L(t) = \int_0^{\infty} f(d) e^{-d(t-T)} dd - \int_0^{\infty} f(d) e^{-dt} dd = \int_0^{\infty} f(d) (1 - d\varepsilon) dd -$$

$$\int_0^\infty f(d)e^{-dT}(1-d\varepsilon)dd = 1 - \int_0^\infty f(d)e^{-dT}dd - \varepsilon \left[\bar{d} - \int_0^\infty df(d)e^{-dT}dd \right] =$$

$$L(T) - \varepsilon L(T) \left[\frac{\bar{d} - \int_0^\infty df(d)e^{-dT}dd}{1 - \int_0^\infty f(d)e^{-dT}dd} \right], \quad (\text{S.4})$$

where $L(T) = 1 - \int_0^\infty f(d)e^{-dT}dd$. Then the initial per capita rate of loss of labeled DNA, d^* , can be calculated for short and long labeling periods. For short labeling periods $T \rightarrow 0$, and we find

$$d^* = \frac{\bar{d} - \int_0^\infty df(d)e^{-dT}dd}{1 - \int_0^\infty f(d)e^{-dT}dd} = \frac{\bar{d} - \int_0^\infty df(d)(1-dT)dd}{1 - \int_0^\infty f(d)(1-dT)dd} = \frac{\overline{d^2}}{\bar{d}} = \bar{d} + \frac{\text{var}(d)}{\bar{d}}, \quad (\text{S.5})$$

where $\text{var}(d) = \overline{d^2} - (\bar{d})^2$ is the variance of the turnover rates in the population. When the labeling period is long, $T \rightarrow \infty$, the per capita rate of label loss is

$$d^* = \frac{\bar{d} - \int_0^\infty df(d)e^{-dT}dd}{1 - \int_0^\infty f(d)e^{-dT}dd} = \bar{d}, \quad (\text{S.6})$$

since all terms $e^{-dT} \rightarrow 0$ as $T \rightarrow \infty$. This confirms the conjecture of Asquith et al. (10) that d^* should approach the average rate of turnover after long labeling period. We now add that the maximal difference between the average turnover rate, \bar{d} , and the loss rate of labeled cells, d^* , is set by the distribution of turnover rates in the population.

5.2 Particular solutions of the kinetic heterogeneity model

For several simple distributions of the turnover rates, we can obtain analytical solutions for the change in the fraction of labeled DNA during the labeling experiment.

Exponential distribution. In this case $f(d) = (1/\bar{d})e^{-d/\bar{d}}$, where \bar{d} is the average turnover rate in the population. Using eqn. (S.1) and (S.2), we find

$$L(t) = 1 - \frac{1}{\bar{d}} \int_0^\infty e^{-dt-d/\bar{d}} dd = 1 - \frac{1}{(t+1/\bar{d})\bar{d}} = \frac{dt}{1+dt}, \quad t \leq T, \quad (\text{S.7})$$

$$\begin{aligned}
L(t) &= \frac{1}{\bar{d}} \int_0^\infty e^{-d(t-T)-d/\bar{d}} dd - \frac{1}{\bar{d}} \int_0^\infty e^{-dt-d/\bar{d}} dd = \frac{1}{1 + \bar{d}(t-T)} - \frac{1}{1 + \bar{d}t} \\
&= L(T) \frac{1 + \bar{d}T}{(1 + \bar{d}t)(1 + \bar{d}(t-T))}, \quad t > T.
\end{aligned} \tag{S.8}$$

When $\bar{d}t \ll 1$, the fraction of labeled DNA is simply $L(t) \approx \bar{d}t$, i.e., the initial rate of increase is again given by the average turnover rate \bar{d} . The initial rate of decline during delabeling is less clear. Let us define $t = T + \varepsilon$ where $\bar{p}\varepsilon \ll 1$. Then after cessation of label administration, using Taylor's expansion we find

$$\begin{aligned}
L(t) &= \frac{1}{1 + \bar{d}\varepsilon} - \frac{1}{1 + \bar{d}T + \bar{d}\varepsilon} = 1 - \bar{d}\varepsilon - \frac{1}{1 + \bar{d}T} + \frac{\bar{d}\varepsilon}{(1 + \bar{d}T)^2} + o(\varepsilon) = \\
&= L(T) - L(T)\bar{d} \left(1 + \frac{1}{1 + \bar{d}T}\right) \varepsilon + o(\varepsilon)
\end{aligned} \tag{S.9}$$

where $L(T) = 1 - 1/(1 + \bar{d}T)$. This expression shows that the initial per capita rate of loss of labeled DNA, $d^* = \bar{d} \left(1 + \frac{1}{1 + \bar{d}T}\right)$, decreases with increasing length of the labeling period (10). If $\bar{d}T \ll 1$ (short labeling), the initial per capita decay rate is $d^* \approx 2\bar{d}$.

Gamma distribution. In this case $f(d) = \lambda(\lambda d)^{k-1}e^{-\lambda d}/(k-1)!$, where λ and k are the scale and shape parameters, respectively, and the average rate of cell turnover $\bar{d} = k/\lambda$, $\sigma_d^2 = \bar{d}^2/k$, and $CV = \sigma_d/\bar{d} = 1/\sqrt{k}$. Note that when $k = 1$, the gamma distribution is identical to the exponential distribution. Substituting the gamma distribution in eqn. (S.1), we find

$$\begin{aligned}
L(t) &= 1 - \frac{\lambda^k}{(k-1)!} \int_0^\infty d^{k-1} e^{-dt-\lambda d} dd \\
&= 1 - \frac{\lambda^k}{(k-1)!(t+\lambda)^k} \int_0^\infty d^{k-1} (t+\lambda)^k e^{-d(t+\lambda)} dd \\
&= 1 - \frac{\lambda^k}{(t+\lambda)^k} = 1 - \left[1 + \frac{\bar{d}t}{k}\right]^{-k}, \quad t \leq T.
\end{aligned} \tag{S.10}$$

Using eqn. (S.2) and proceeding similarly, we find the change in the fraction of labeled DNA during delabeling:

$$L(t) = \left[1 + \frac{\bar{d}(t-T)}{k}\right]^{-k} - \left[1 + \frac{\bar{d}t}{k}\right]^{-k}, \quad t > T. \tag{S.11}$$

(S.12)

The initial rate of increase in the fraction of labeled cells is also independent of the length of the labeling period and, initially, for $t = \varepsilon$ (such as $\bar{d}\varepsilon \ll 1$) is

$$L(\varepsilon) = 1 - \left[\frac{1}{1 + \frac{\bar{d}\varepsilon}{k}} \right]^k = 1 - (1 - k\bar{d}\varepsilon/k) + o(\varepsilon) = \bar{d}\varepsilon + o(\varepsilon). \quad (\text{S.13})$$

as expected. The initial per capita rate of loss of labeled DNA is somewhat more complex. For times $t = T + \varepsilon$ such as $\bar{d}\varepsilon \ll 1$, using Taylor's expansion, we find

$$L(t) = \left[1 + \frac{\bar{d}\varepsilon}{k} \right]^{-k} - \left[1 + \frac{\bar{d}(T + \varepsilon)}{k} \right]^{-k} = 1 - \frac{1}{\left(1 + \frac{\bar{d}T}{k} \right)^k} - \bar{d}\varepsilon \left[1 - \frac{1}{\left(1 + \frac{\bar{d}T}{k} \right)^k} \right] \quad (\text{S.14})$$

It is useful to rewrite this expression in terms of $L(T)$:

$$L(t) = L(T) - L(T) \frac{\bar{d}\varepsilon}{1 + \bar{d}T/k} \left[\frac{(1 + \bar{d}T/k)^{k+1} - 1}{(1 + \bar{d}T/k)^k - 1} \right] = L(T)(1 - d^*\varepsilon). \quad (\text{S.15})$$

where $d^* = \frac{\bar{d}}{1 + \bar{d}T/k} \left[\frac{(1 + \bar{d}T/k)^{k+1} - 1}{(1 + \bar{d}T/k)^k - 1} \right]$ is the initial per capita loss of labeled DNA. For short labeling ($\bar{d}T \ll 1$), the initial per capita decay rate is $d^* \approx \bar{d}(k + 1)/k$, and as the shape parameter k becomes larger, the decline rate d^* approaches the average proliferation rate \bar{d} . For long labeling periods ($\bar{d}T \gg 1$), $d^* \approx \bar{d}$, as expected.

Truncated gamma distribution. Under some circumstances the distribution of turnover rates may allow for too high rates of cell turnover. To circumvent this problem one may use a truncated distribution. For a gamma distribution truncated at maximal value d_{max} , the distribution is similar as above with an added normalization constant C , $f(d) = C^{-1}\lambda(\lambda d)^{k-1}e^{-\lambda d}/(k-1)!$. The constant C is found by normalizing the probability distribution

$$C = \int_0^{d_{max}} f(d) dd = 1 - \frac{\Gamma(k, d_{max}\lambda)}{(k-1)!}, \quad (\text{S.16})$$

where $\Gamma(k, d) = \int_d^\infty x^{k-1} e^{-x} dx$ is an incomplete gamma function. The average turnover rate then has to be calculated numerically

$$\bar{d} = C^{-1} \int_0^{d_{max}} df(d) dd = \frac{k}{\lambda} \left[\frac{1 - \frac{\Gamma(k+1, d_{max}\lambda)}{k!}}{1 - \frac{\Gamma(k, d_{max}\lambda)}{(k-1)!}} \right]. \quad (\text{S.17})$$

For the fraction of labeled nucleotides, we proceed as in eqn. (S.10) and obtain

$$\begin{aligned} L(t) &= 1 - \frac{\lambda^k}{C(k-1)!} \int_0^{d_{max}} d^{k-1} e^{-dt-\lambda d} dd \\ &= 1 - \frac{\lambda^k}{C(k-1)!(t+\lambda)^k} \int_0^{d_{max}(t+\lambda)} x^{k-1} e^{-x} dx \\ &= 1 - \frac{\lambda^k}{C(k-1)!(t+\lambda)^k} \left[(k-1)! - \int_{d_{max}(t+\lambda)}^\infty x^{k-1} e^{-x} dx \right] \\ &= 1 - \frac{\lambda^k}{(t+\lambda)^k} \times \frac{(k-1)! - \Gamma(k, d_{max}(\lambda+t))}{(k-1)! - \Gamma(k, d_{max}\lambda)}, \quad t \leq T. \end{aligned} \quad (\text{S.18})$$

During delabeling ($t > T$), we proceed as in eqn. (S.11) and find

$$\begin{aligned} L(t) &= \frac{\lambda^k}{(\lambda+t-T)^k} \times \frac{(k-1)! - \Gamma(k, d_{max}(\lambda+t-T))}{(k-1)! - \Gamma(k, d_{max}\lambda)} - \\ &\quad \frac{\lambda^k}{(t+\lambda)^k} \times \frac{(k-1)! - \Gamma(k, d_{max}(\lambda+t))}{(k-1)! - \Gamma(k, d_{max}\lambda)}. \end{aligned} \quad (\text{S.19})$$

Since $\lim_{d_{max} \rightarrow \infty} \Gamma(k, d_{max}) = 0$, at $d_{max} \rightarrow \infty$,

the fraction of labeled nucleotides becomes identical to eqn. (4) with $\lambda = k/\bar{d}$.

5.3 Non-parametric estimates of the distribution of proliferation rates in the population

Mathematically, the last term in eqn. (S.1) is a Laplace transformation of $f(p)$. This result stems from the assumption of exponentially distributed inter-division times of cells and raises

the intriguing possibility that from the change in the fraction of labeled DNA during label administration, one can estimate the distribution of proliferation rates in the population. Let us denote $f^*(t)$ as the Laplace transformation of $f(d)$:

$$f^*(t) = \mathcal{L}[f(d)] = \int_0^\infty f(d)e^{-dt}dd. \quad (\text{S.20})$$

From eqn. (S.1), one finds the distribution of proliferation rates in the population using the inverse Laplace transformation:

$$f(d) = \mathcal{L}^{-1}[1 - L(t)]. \quad (\text{S.21})$$

where $L(t)$ is a curve describing the change of the fraction of labeled DNA during label administration. Such a curve could be obtained in several ways, for example, by interpolating the data. Application of this method for the analysis of experimental data will be published elsewhere.

Data fitted with:		Data generated using:					
		Gamma model		Exponential model		Two-populations model	
		7 days	15 days	7 days	15 days	7 days	15 days
Asymptote	\bar{d}	0.076 0.068—0.085	0.068 0.06—0.077	0.082 0.073—0.096	0.08 0.07—0.092	0.04 0.034—0.046	0.039 0.032—0.047
	d	0.121 0.105—0.14	0.117 0.099—0.137	0.203 0.17—0.238	0.199 0.169—0.231	0.052 0.04—0.066	0.054 0.038—0.071
Exponential	\bar{d}	0.09 0.082—0.104	0.09 0.076—0.1	0.11 0.105—0.122	0.12 0.104—0.137	0.05 0.042—0.055	0.05 0.040—0.055
	α	0.83 0.773—0.908	0.76 0.70—0.82	0.51 0.488—0.536	0.48 0.456—0.51	1 0.857—1.0	1 0.835—1.0
Gamma	\bar{d}	0.097 0.085—0.112	0.099 0.085—0.117	0.154 0.14—0.169	0.197 0.152—0.271	0.044 0.038—0.052	0.044 0.036—0.054
	k	0.594 0.478—0.768	0.44 0.367—0.536	0.197 0.184—0.211	0.159 0.134—0.183	1.329 0.796—2.947	1.132 0.679—2.901

Table 1: Estimates of the parameters after fitting three models to three sets of artificial data. Rows correspond to different models used to fit the data, and columns correspond to the models used to generate the data. We show parameter estimates of the Asymptote model, the Exponential model (in which a fraction α of cells have exponentially distributed turnover rates), and the Gamma model (with gamma distributed turnover rates). Data were generated using the Gamma model (eqn. (4)), the Exponential model (eqn. (8)), and the Two-populations model (eqn. (2)). The 95% confidence intervals, that are shown below the mean values, were obtained by bootstrapping the residuals with 1000 simulations. Data have been generated for two labeling periods, of 7 and 15 days, respectively. For all data, the average rate of turnover was fixed at 0.1/day. Other parameters used to generate the data are: $k = 0.5$ (Gamma model), $\alpha = 0.5$ and $\bar{d}_\alpha = 0.2/\text{day}$ (Exponential model), $d_1 = 1/\text{day}$, and $\alpha = 0.07$ (Two-populations model).

	Data fitted with:		
	Asymptote model	Exponential model	Gamma model
$d/\bar{d}_\alpha/k$	2.87 (2.22—3.65)	1.94 (1.46—2.6)	0.12 (0.09—0.17)
$\bar{d}_1, \% \text{ day}^{-1}$	0.57 (0.5—0.67)	0.59 (0.51—0.7)	0.62(0.53—0.78)
\bar{d}_2	0.41 (0.34—0.5)	0.44 (0.36—0.53)	0.43 (0.34—0.54)
\bar{d}_3	0.38 (0.31—0.47)	0.41 (0.33—0.5)	0.37 (0.27—0.48)
\bar{d}_4	0.41 (0.33—0.5)	0.44 (0.36—0.54)	0.43 (0.32—0.57)
$\tau_1, \text{ day}$	1. (0.91—1.51)	1. (0.93—1.53)	1. (0.93—1.57)
τ_2	0.78 (0.28—1.)	0.81 (0.35—1.)	0.8 (0.31—1.)
τ_3	1.97 (1.—2.65)	2.06 (1.14—2.7)	1.87 (0.73—2.67)
τ_4	1.7 (0.98—2.45)	1.83 (1.—2.54)	1.79 (1.—2.58)
RSS, 10^{-3}	6.19	5.94	5.87

Table 2: Average turnover rates of CD4⁺ T cells from four healthy humans as estimated by fitting the data from Mohri et al. (2) using the Asymptote model, the Exponential model, and the Gamma model. The best fits of the models resulted in different average rates of cell turnover \bar{d}_i and initial delays of labeling τ_i . Other parameters, that could be assumed to be identical between different patients, are the death rate of labeled cells d (Asymptote model), the rate of turnover \bar{d}_α of the turning-over sub-population in the Exponential model, and the shape parameter k in the model with gamma distributed turnover rates. For the model with gamma distributed turnover rates, an asymptote level $\alpha = 1$ provided the best fit of the data. The quality of the fit is illustrated by the residual sum of squares (RSS). The 95% confidence intervals were obtained by bootstrapping the residuals with 1000 simulations.

	Data fitted with:		
	Asymptote model	Exponential model	Gamma model
$\alpha_1/\alpha/k_1$	0.08 (0.07—0.10)	0.13 (0.12—0.16)	0.033 (0.028—0.039)
$\alpha_2/\alpha/k_2$	0.13 (0.09—0.73)	0.13 (0.12—0.16)	0.116 (0.066—0.341)
$\alpha_3/\alpha/k_3$	0.26 (0.10—1.0)	0.13 (0.12—0.16)	0.347 (0.099— 10^7)
$\alpha_4/\alpha/k_4$	0.10 (0.07—0.28)	0.13 (0.12—0.16)	0.082 (0.05—0.155)
\bar{d}_1 , % per day	0.36 (0.31—0.43)	0.48 (0.39—0.57)	0.62 (0.53—0.71)
\bar{d}_2	0.23 (0.18—0.30)	0.27 (0.21—0.34)	0.23 (0.19—0.28)
\bar{d}_3	0.21 (0.17—0.31)	0.29 (0.22—0.39)	0.2 (0.17—0.27)
\bar{d}_4	0.22 (0.18—0.3)	0.24 (0.2—0.32)	0.23 (0.19—0.28)
τ_1	0.99 (0.73—1.38)	1.76 (1.33—1.95)	1.89 (1.75—1.98)
τ_2	0.65 (0.—0.94)	0.76 (0.11—0.99)	0.65 (0.28—0.92)
τ_3	0.85 (0.—1.99)	1.73 (0.59—2.4)	0.82 (0.—1.81)
τ_4	0. (0.—0.63)	0. (0.—0.64)	0. (0.—0.55)
RSS, 10^{-3}	3.4	3.85	1.56

Table 3: Average turnover rates of CD8⁺ T cells from four healthy humans as estimated by fitting the data from Mohri et al. (2) using the Asymptote model, the Exponential model and the Gamma model. The best fits of the models resulted in different parameter estimates for all patients, with the exception of the fraction of turning over cells α in the Exponential model (which was fitted as one parameter for all patients). As for CD4⁺ T cells, in the model with gamma distributed turnover rates, the asymptote level $\alpha = 1$ provided the best fit of the data. The shown 95% confidence intervals were obtained by bootstrapping the residuals with 1000 simulations.

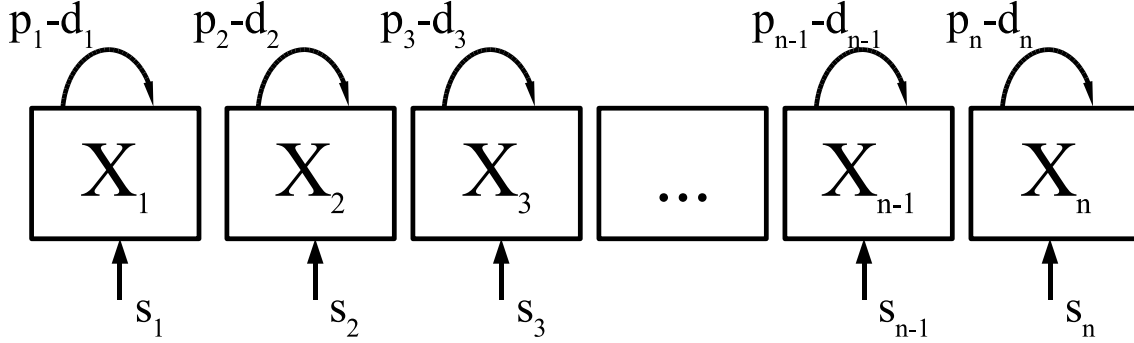


Figure 1: A cartoon of the model with explicit kinetic heterogeneity. In the model, the population of cells consists of n sub-populations with different rates of turnover. In the i^{th} sub-population, there is a source of new cells that enter the cell population at rate s_i cells per day, cells divide at rate p_i per day, and die at rate d_i per day. To maintain the size of all sub-populations constant, $d_i - p_i = s_i/X_i$ for every sub-population i , where X_i is the number of cells in the i^{th} sub-population. In this model we assume that the source produces only labeled cells during the labeling phase, and delabeled cells during the unlabeling phase (11).

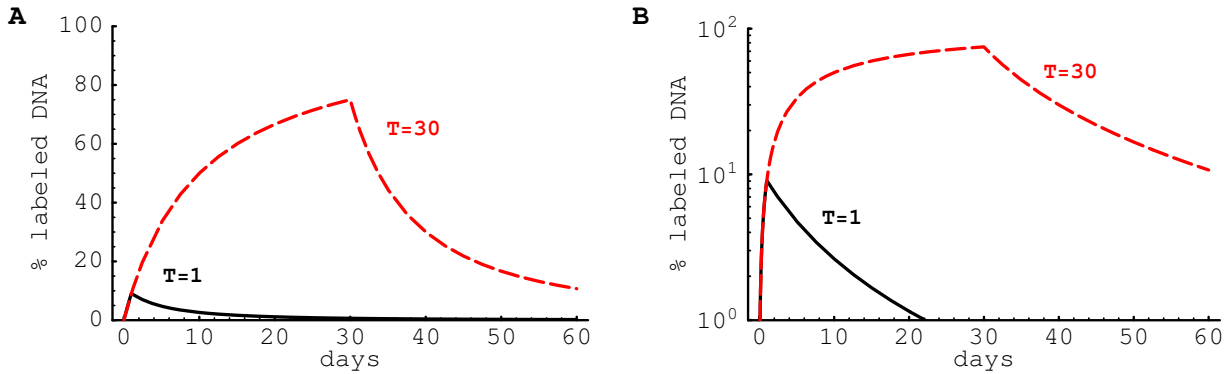


Figure 2: Model predictions for exponentially distributed turnover rates. We have plotted the changes in the fraction of labeled DNA according to the explicit kinetic heterogeneity model with exponentially distributed turnover rates (eqn. (5), mean $\bar{d} = 0.1/\text{day}$). Predicted changes are shown for a short labeling period ($T = 1$ day, solid line) and a long labeling period ($T = 30$ days, dashed line) on a linear (panel A) and a logarithmic (panel B) scale. The initial uplabeling rate is independent of the length of the labeling period and is given by \bar{d} . The initial rate of delabeling, in contrast, depends on the length of the labeling period and is approximately twice as fast in the case of short-term labeling as compared to long-term labeling.

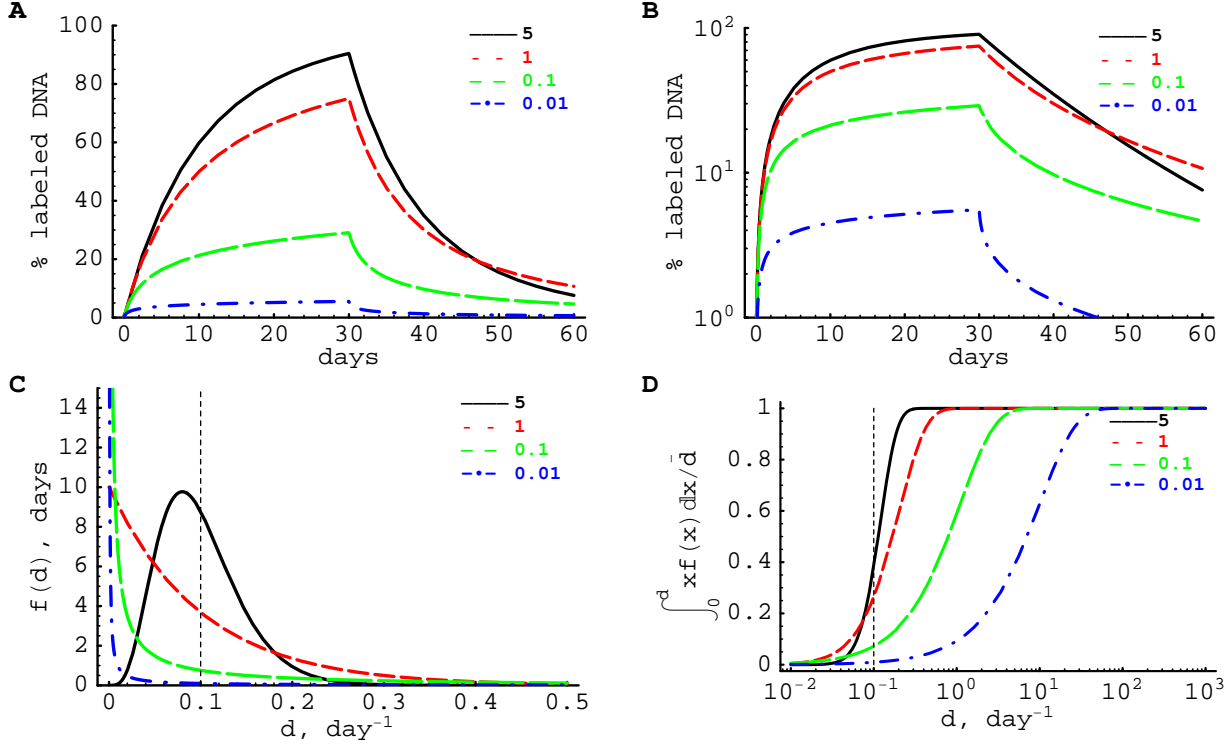


Figure 3: Model predictions for gamma-distributed turnover rates. We have plotted the changes in the fraction of labeled DNA according to the kinetic heterogeneity model with gamma-distributed turnover rates (eqn. (4)) with average turnover rate $\bar{d} = 0.1/\text{day}$ on a linear (panel A) or logarithmic (panel B) scale. Predicted changes are shown for different values of the shape parameter k . Larger values of k correspond to a more symmetric distribution (Panel C). For low values of the shape parameter k , the loss of labeled DNA after label cessation is biphasic, which is most clearly visible on a logarithmic scale for $k < 1$ (panel B). This characteristic of the kinetic heterogeneity model differs from the Asymptote models which have a constant *per capita* rate at which labeled DNA is lost. Note that for shape parameters $k < 1$, the distribution of turnover rates $f(d)$ becomes extremely skewed with most cells undergoing hardly any division and relatively few cells undergoing extremely many rounds of division (panel C). Panel D gives the cumulative contribution of sub-populations with a particular turnover rate d to the average rate of turnover of the population \bar{d} . The vertical line shows the value of the average proliferation rate \bar{d} . For high values of the shape parameter ($k = 5$), the cell sub-populations with turnover rates that are somewhat lower or higher than \bar{d} give the main contribution to the average turnover rate. In contrast, for low values of k ($k = 0.01$), the major contribution to the average turnover rate comes from sub-populations with extremely rapid turnover rates ($d \gg \bar{d}$); about 50% of the average turnover is due to a few sub-populations with turnover rates that exceed 10 per day, which is biologically unrealistic.

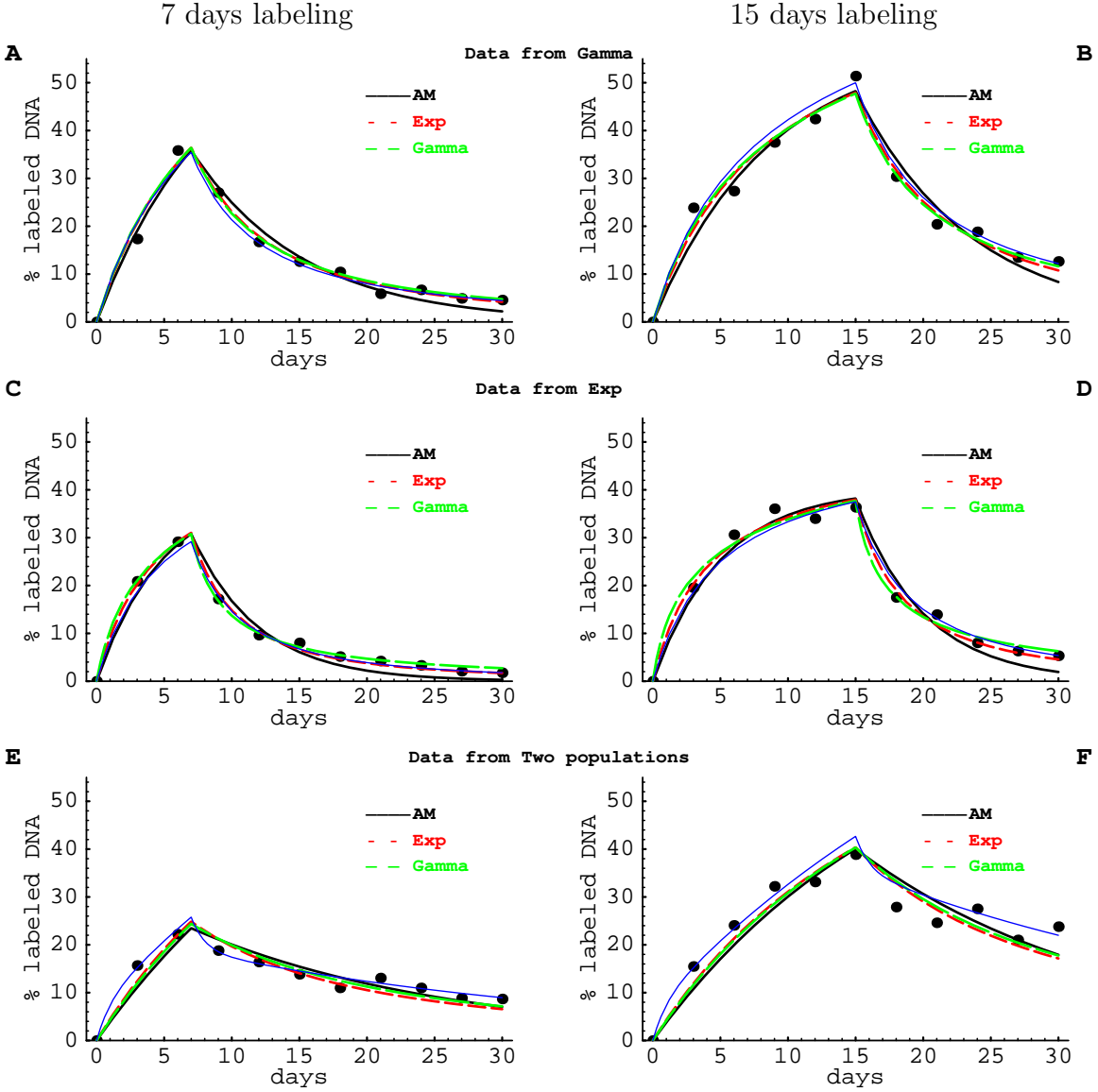


Figure 4: Fitting artificial data (black dots) with the Asymptote model (eqn. (1), solid black lines), the Exponential model, in which a fraction α of the cells have exponentially distributed turnover rates (eqn. (8), small red dashed lines), and the Gamma model with gamma distributed turnover rates (eqn. (4), large green dashed lines). Data were generated using the Gamma model (panel A&B), the Exponential model (panel C&D) and the Two-populations model (panel E&F, eqn. (2)), respectively. Thin blue lines show the exact curves of the models that were used to generate the data. The different models were fitted to 11 datapoints taken from these predicted curves after having added noise to these data points. Noise was added by a relative change of the predicted value with a normally distributed error (with standard deviation of the distribution $\sigma = 0.1$). The models were fitted to data from artificial labeling experiments in which the label was administered for 7 (left panels) or 15 (right panels) days. Parameter estimates providing the best fit are shown in Table 1, and the corresponding estimates of the average rates of cell turnover \bar{d} are shown in Figure 5. Parameters used to generate the data are also given in Table 1.

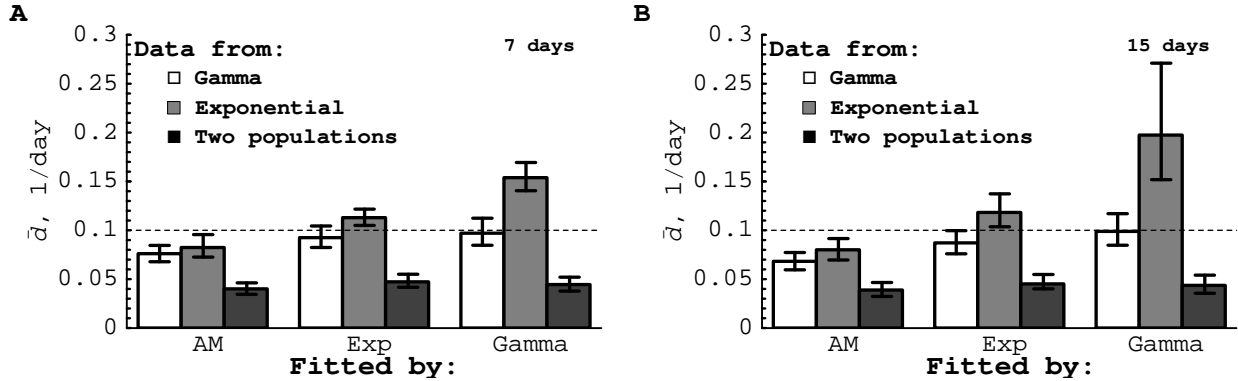


Figure 5: By fitting the artificial data described in the text, we estimated the average turnover rate using three models: the Asymptote model (eqn. (1)), the Exponential model (in which a fraction α of cells have exponentially distributed turnover rates, eqn. (8)), and the Gamma model (with gamma-distributed turnover rates, eqn. (4)). Estimated mean values and 95% confidence intervals obtained by bootstrapping the residuals with 1000 simulations are shown. Data were generated using the Gamma model (\square), the Exponential model (\blacksquare) and the Two-populations model (\blacksquare). Labeling periods were 7 (panel A) and 15 (panel B) days. Horizontal dashed lines denote the actual average rate of lymphocyte turnover in all data, $\bar{d} = 0.1/\text{day}$. Note that in this example, the Asymptote model always underestimated the average rate of cell turnover, and that there is a systematic 2-fold underestimation of the average turnover by all models when the data from the Two-populations model were fitted. This is because all three models fail to describe the relatively rapid accumulation of the label at early time points (see Figure 4E–F).

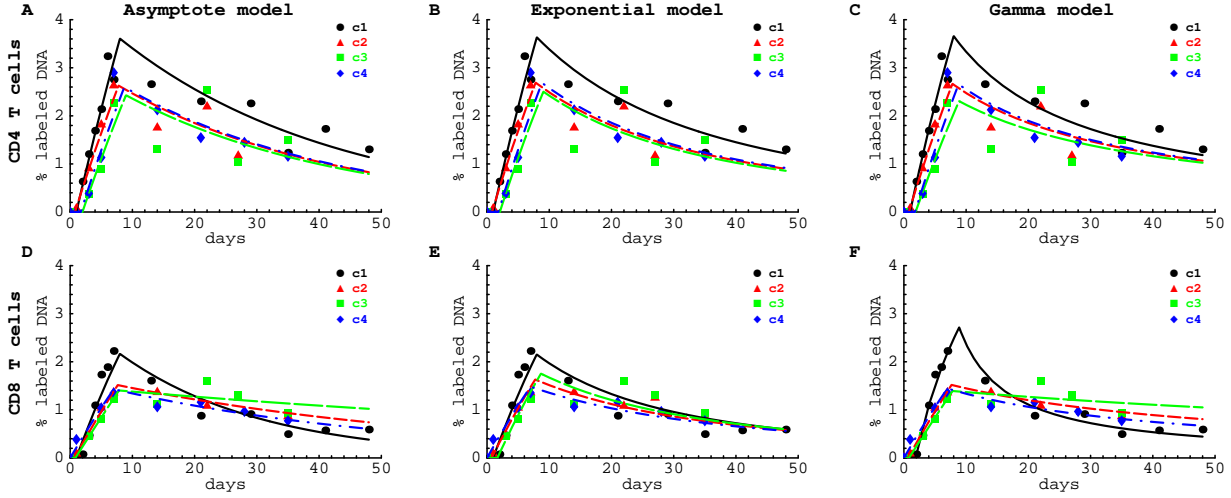


Figure 6: Fitting the deuterium labeling data of $CD4^+$ (top rows) and $CD8^+$ (bottom rows) T cells in four healthy humans with three models: the Asymptote model (panels A and D), the Exponential model, in which a fraction α of cells have exponentially-distributed turnover rates (eqn. (8), panels B and E), and the Gamma model, with gamma-distributed turnover rates (eqn. (4), panels C and F). Experimental data obtained from Mohri et al. (2) are shown as symbols and the curves are the best model fits. The sum of squared residuals of the model fits to the data on the dynamics of $CD4^+$ T cells are $(6.19, 5.94, 5.87) \times 10^{-3}$ for the Asymptote model, the Exponential model and the Gamma model, respectively. The sum of squared residuals of the model fits to the data on the dynamics of $CD8^+$ T cells are $(3.4, 3.85, 1.56) \times 10^{-3}$ for the Asymptote model, the Exponential model and the Gamma model, respectively. Note that the two explicit kinetic heterogeneity models describe these data with similar (Exponential model) or even better (Gamma model) quality compared to the Asymptote model.

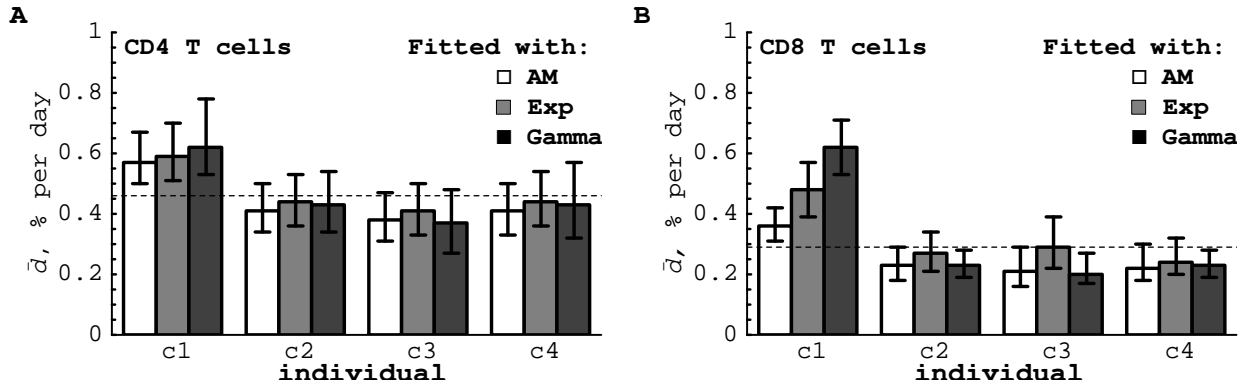


Figure 7: Estimates of the average turnover rates of CD4⁺ (panel A) and CD8⁺ (panel B) T cells in four healthy humans obtained by fitting with three different models: the Asymptote model (□), the Exponential model (■), in which a fraction α of the cells have exponentially-distributed turnover rates, and the Gamma model (■) with gamma-distributed turnover rates. Best fits of the data are shown in Figure 6, and estimates of all parameters of the models are shown in Appendix (Table 2 and 3). Confidence intervals were obtained by bootstrapping the residuals with 1000 simulations. Horizontal dashed lines denote the mean of the estimated turnover rates in all patients and all models for CD4⁺ ($\bar{d} = 0.46\%$ per day) and CD8⁺ ($\bar{d} = 0.29\%$ per day) T cells. Note that all models deliver very similar estimates for the average turnover rate \bar{d} , with the exception of the estimated CD8⁺ T-cell turnover rates in individual c1 which are highly model-dependent.